Accepted for presentation in: VDE-ITG Conference on Mobile Communications (MKT), Osnabrück, Germany, May 2026

Reflection Instead of Densification: Experimental Insights into IRS-Aided Industrial 6G mmWave

Marco Danger, Simon Häger, Christian Arendt, Florian Schmickmann, Marcel Kaudewitz, Stefan Böcker, and Christian Wietfeld
Communication Networks, TU Dortmund University, 44227 Dortmund, Germany
E-mail: {Marco.Danger, Simon.Haeger, Christian.Arendt, Florian.Schmickmann, Marcel.Kaudewitz, Stefan.Boecker, Christian.Wietfeld}@tu-dortmund.de

***Abstract*—Millimeter-Wave (mmWave) communication is a key enabler of advanced wireless capabilities in future private 6G networks, particularly within industrial contexts. While mmWave offers access to large bandwidths, its performance is constrained under Non-Line-of-Sight (NLOS) conditions, especially in cluttered Indoor Factory (InF) settings. Although network densification through additional cells can significantly improve coverage and capacity, it also increases energy consumption, infrastructure complexity, and associated costs. This work investigates the application of the 6G technology concept of passive Intelligent Reflecting Surfaces (IRSs), in the form of the static-passive HELIOS and reconfigurable, semi-passive R-HELIOS IRS panels as an efficient method to realize qualitative mmWave coverage. We experimentally assess their ability to compensate for the deactivation of a mmWave cell by introducing strong artificial reflection paths leading to Line-of-Sight (LOS)-like connectivity. Measurements using commercial cellular equipment show that static HELIOS IRSs enhance received power and data rates in preselected NLOS regions, reaching a peak of 11 dB and 552 Mbit/s in a multi-user scenario. The R-HELIOS IRS with Ultra-Wideband (UWB)-enabled beam steering further supports adaptive beam focusing, maintaining downlink throughputs of at least 900 Mbit/s for a mobile user in NLOS, while consuming power contrary to static reflectors, but achieving a significant reduction in overall power consumption compared to an additional cell. Importantly, our results underscore the potential of IRS-assisted 6G networks to exhibit a reduced mmWave cell density without compromising link performance, offering a more efficient network operation.**

***Video Abstract*—Visual documentation can be accessed on http://tiny.cc/ITGDanger**

I. IRS-aided Cell Reduction for Private mmWave

The integration of mmWave communication into future 6G networks aims to meet the stringent performance requirements of industrial environments through large bandwidths and resulting high data rates. However, the vulnerability of mmWave signals to blockage and rapid degradation in NLOS conditions remains a major challenge [1]. Whereas network densification with additional cells can mitigate these effects, it increases energy consumption and operational complexity. As an efficient alternative, IRSs have emerged as a hot-topic in contemporary 6G research to enhance wireless propagation in shadowed areas, either *with* (semi-passive IRS) or *without* (static-passive IRS) power consumption, compared to full-blown active base stations [2]. As illustrated in Fig. 1, strategically placed reflectors can jointly substitute the coverage of an additional mmWave cell, enabling both static and mobile devices to achieve LOS-like performance under diverse radio conditions.

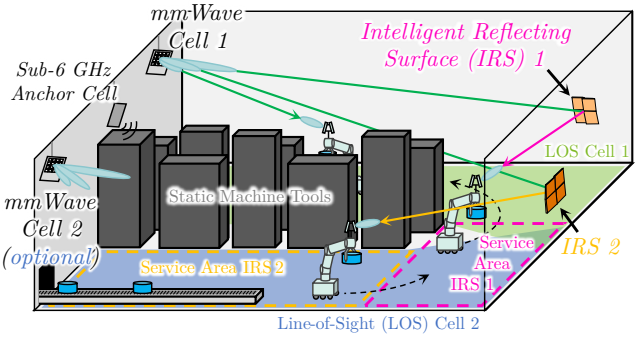

Fig. 1: Strategically designed and placed IRSs create reflection paths for LOS-like performance, enabling robust connectivity in NLOS with fewer cells.

The evaluated approaches differ primarily in their balance between capacity, coverage, energy demand, cost and complexity, as summarized qualitatively in Tab. I. Adding an additional cell provides the highest capacity and coverage but results in increased energy consumption and maintenance overhead. In contrast, a static-passive IRS offers a sustainable coverage enhancement within its predefined service area at minimal cost. The reconfigurable semi-passive IRS extends this concept by dynamically adapting its reflection pattern based on Radio Access Technology (RAT)-external or -internal positioning data, enabling improved coverage in highly dynamic scenarios with moderate energy demand [3, 4]. These qualitative distinctions between additional cell and IRS variants are validated through a series of experiments conducted in this work.

TABLE I: Experimental evaluation in this work: Comparison of additional cell and IRS-based extension of mmWave connectivity into NLOS regions.

Solution		Capacity	Coverage	Energy demand	Cost	Complexity
Additional cell		++	++	--	--	--
Static-passive IRS		(+)*	+	++	++	++
Reconfig. semi-passive IRS	RAT-external steering (UWB)	+	++	+	○	+
	RAT-internal steering	+	++	++	+	○

Note: *: If active UE is present in preconfigured service area of IRS
Legend: ++ (strongly beneficial) to -- (strongly detrimental)
Highlighting: In This Work and Future 6G Perspective

The remainder of this work is structured as follows. Current advances in the utilization of mmWave and various IRS types are the subject of Sec. II. In Sec. III, the baseline performance of a private multi-cell mmWave network is first examined, after which the Key Performance Indicator (KPI) monitoring and control system is presented, which is utilized to evaluate three further scenarios with a single mmWave cell and various reflectors, so-called Holistic Enlightening of bLackspots with passIve reflectOr moduleS (HELIOS) [5]. Subsequently, in Sec. IV, the results obtained are analyzed and the IRS's impact is evaluated. Finally, the findings of this work are summarized.

II. Advances in mmWave and IRS Deployments

The restricted coverage by mmWave frequencies is based on high path losses as well as blocking and scattering caused by obstacles within the radio environment. Researchers are addressing these limitations through approaches such as adaptive beam steering, intelligently designed and placed reflective surfaces or relay stations, such as those evaluated in [6]. Building on the potential of mmWave technology, increasing energy efficiency has emerged as a critical priority for future networks [7]. To enable efficient and scalable 6G systems, future mmWave deployments must adopt robust optimization strategies that reduce emissions and operational costs without compromising performance. To support mobile industrial scenarios, mmWave communication must be supplemented with dynamic adaptation strategies that counteract frequent signal disruptions caused by mobility and complex environments. A promising approach is presented in [8], where location-aware beam switching effectively enhances link stability in a realistic industrial setting.

Another method to support mobile use cases involves reconfigurable IRSs, which can operate based on both RAT-external and RAT-internal information. While this work evaluates a UWB-driven semi-passive IRS following a RAT-external approach (cf. Tab. I), future 6G systems also aim to integrate accurate RAT-internal positioning and sensing, enabling more efficient IRS operation without external support [9]. Moreover, user-, reflector-, and cell-side Channel State Information (CSI)-driven beam management is envisioned for IRS-assisted 6G communication, although these mechanisms remain open research topics and are not yet standardized [10, 11]. To the best of the authors' knowledge, a full RAT-internal integration of these functionalities into cellular systems has not yet been realized [3, 12], but could be trialed in future using Open RAN-driven 6G testbeds. In summary, Tab. 1 in [4] provides a comprehensive survey of experimentally evaluated IRS implementations, highlighting the diversity of current design approaches.

This work presents an empirical study aimed at evaluating both static and reconfigurable IRS technologies as enablers of reliable and more efficient mmWave connectivity in InF settings. In contrast to a previous study, in which the energy efficiency of mobile User Equipments (UEs) was optimized [13], a more efficient design of the private network infrastructure is investigated in this work. The goal is to evaluate whether IRSs

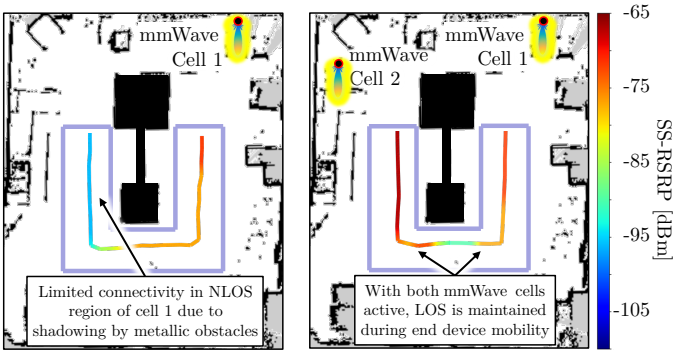

(a) One mmWave cell (b) Two mmWave cells

Fig. 2: REMs of mmWave connectivity in multi-cell network.

can effectively substitute additional mmWave cells, which already consume around 400 W at low (baseline) and 1,100 W at high load (peak) [14], while maintaining high communication quality. A baseline multi-cell mmWave setup is compared against three reduced-cell scenarios, two of which supported by IRSs, and connectivity as well as performance metrics are analyzed. During this process, among other things, the beam-tracking capabilities of a UWB-enabled reconfigurable IRS are assessed during user mobility. By grounding its analysis in real-world measurements, this study contributes to a more practical understanding and evaluation of IRS deployments in future 6G industrial networks.

III. Network Capability and Experimental Layout

This section describes the network components deployed to carry out the subsequent experiments. First, the baseline capability of the deployed private network is presented. Subsequently, the static and mobile devices are introduced, that are based on the Spatially distributed Traffic and Interference Generation (STING) concept [15] and whose measurements are utilized for active as well as passive KPI monitoring. Next, the design of two static reflectors, which are configured for fixed service areas, is described. Finally, semi-passive Reconfigurable HELIOS (R-HELIOS) and its UWB-based reflection beam steering is introduced.

TABLE II: Configuration of 5G NSA / EN-DC mobile network.

	Parameter	Description/Value
Cell Configuration	**FR1 / LTE Anchor Cell**	
	Frequency Band	LTE band 7 (FDD)
	Center Frequency	2.65 and 2.53 GHz (DL/UL)
	Bandwidth	20 MHz
	Transmit Power	100 mW (EIRP)
	FR2 / NR mmWave Cells	
	Frequency Band	5G NR n257 (TDD)
	Frequency Range	26.7 to 27.5 GHz
	TDD Pattern	DDSU
	Component Carriers (CCs)	8
	Bandwidth	100 MHz per CC
	Subcarrier Spacing (SCS)	120 kHz
	Transmit Power	15 mW (EIRP)
UEs	Device Model	Quectel RG530F-EU
	Modem	Qualcomm SDX65
	mmWave Antenna Module	RA530T with four QTM547 (8×8, cross-polarized)

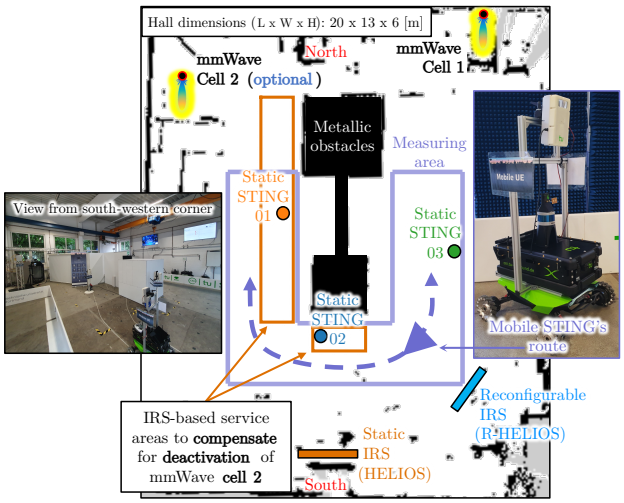

Fig. 3: Top view of measuring environment with network components for evaluating IRS-based reduction of active radio infrastructure (mmWave cell 2).

A. Baseline Performance of Single- and Multi-Cell Network

To evaluate the baseline performance and connectivity of the mmWave network, a mobile STING device is utilized to execute measurements with one and two activated radio units and cells. For comparison of the two configurations, the received power values for the same mobile trajectory are shown in Fig. 2, which also depicts the scanned floor plan of the industrial transfer environment as well as the mmWave cells' positions. In both northern corners of the hall, a mmWave cell is installed at a height of 1.6 m, each facing south and forming the multi-cell network together with a Frequency Range 1 (FR1) anchor cell (cf. Tab. II). The two cells are separated by metallic obstacles, forming two corridors that are connected at the southern end of the hall, creating the U-shaped measuring area.

With only cell 1 active, the shadowing caused by the metallic objects in the center of the measuring area results in a significant deterioration in connectivity compared to the LOS condition in the eastern corridor. The received power drops from a maximum of −70 dBm by 25 dB to −95 dBm in the NLOS area. When mmWave cell 2 is now additionally activated, LOS exists in both corridors, as can be seen in Fig. 2b. With an uninterrupted view to one of the two cells, the mobile device achieves data rates of up to 570 Mbit/s in Uplink (UL) and 1.27 Gbit/s in Downlink (DL) direction.

This evidently demonstrates that adding a mmWave cell significantly improves connectivity in previously shadowed areas but also increases energy use and operating costs. The following experiments investigate whether comparable performance in NLOS conditions can be achieved more efficiently by reduced active radio infrastructure in combination with IRSs.

B. KPI Monitoring with Static and Mobile STING Devices

The various components used for the following experiments are depicted in Fig. 3. Three static STINGs and one mobile STING are placed within the measuring area, whereby all devices are equipped with the same UE (cf. Tab. II) as well as a control unit. The static UEs are located in three different radio conditions: STING 1 in LOS of cell 2, STING 2 in NLOS of cell 1 and 2, and STING 3 in LOS of cell 1. The mobile STING, on the other hand, can be moved freely along the indicated route and thus covers various radio conditions. With the help of the control unit of each UE, the measurement data of all STING devices can be continuously monitored with a time resolution of up to 250 ms, so that impacts caused by environmental changes and mobility can be analyzed. The monitored KPIs relevant for this work include the Synchronization Signal Reference Signal Received Power (SS-RSRP), the Physical Uplink Shared Channel (PUSCH) UE transmit (Tx) power, the data path and data rate in UL and DL directions, both measured simultaneously with *iperf3* [16].

C. Positioning and Design of Static HELIOS Reflectors

In the course of this work, static-passive HELIOS reflectors are deployed, with their position being indicated in Fig. 3. There, two IRSs are placed above each other at heights of 1.2 m and 2.2 m, respectively. To minimize the impact of their mounting on radio propagation, absorbers are installed between and behind the reflectors. The design process [5], which considers the frequency, angle of the incident radio wave (originating from mmWave cell 1) and the specified service area for which the minimum reflection gain is maximized, determines a 2×3 module arrangement with a total size of $29.7\,\mathrm{cm} \times 29.7\,\mathrm{cm}$ for the bottom HELIOS (service area 2) which creates a broadened horizontal reflection beam

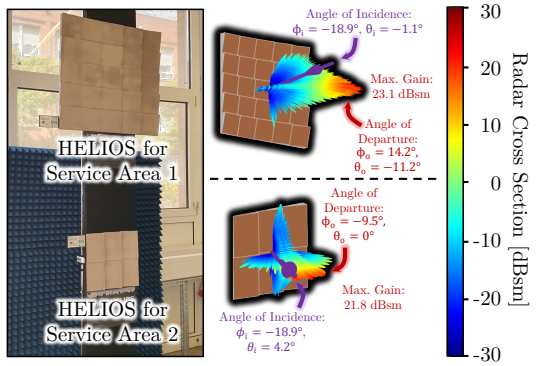

(a) Deployed IRSs and corresponding reflection patterns

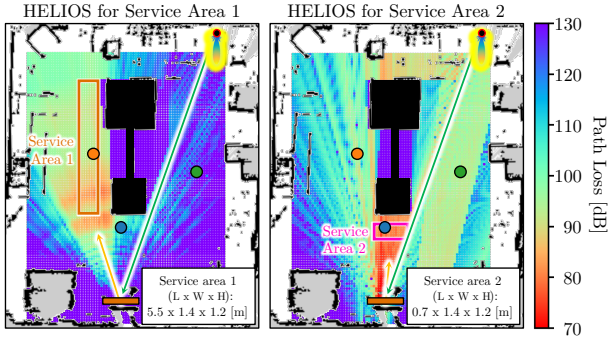

(b) Simulated path loss from each reflector

Fig. 4: Design and simulated impact of used static-passive HELIOS reflectors.

of about 20°. An image of the 3D-printed reflector and the associated reflection pattern in form of the radar cross section is shown in Fig. 4a. The latter also portrays the top HELIOS (service area 1), which consists of 5×5 modules with a total size of $60\,\mathrm{cm} \times 60\,\mathrm{cm}$ which broadens the reflection beam both horizontally and vertically by approximately 24° and 10°, respectively. Expanding the reflection beam in both dimensions accounts for the increased IRS footprint size compared to bottom HELIOS. To illustrate the effectiveness of the two IRSs, their associated radar cross section patterns are utilized as antenna characteristics in ray-tracing simulations with [17], clearly highlighting that they reflect the mmWave cell's incident wave toward the intended service area and vice versa. Their results illustrated in Fig. 4b emphasize that the service area of the bottom HELIOS serves STING device 2 and that of the top HELIOS STING 1.

D. R-HELIOS with UWB-based Reflection Beam Steering

While the static HELIOS IRSs are intentionally designed to create reflection paths to two distinct service areas and static STINGs {01, 02}, the mobile STING is deliberately remote-controlled at walking speed along a 6 m trajectory outside the existing service areas. In order to cover the movement of the mobile UE, several small or one large static IRS would be necessary to serve the large beam widths required. As an alternative solution, R-HELIOS [4] can be introduced into the radio environment. Even though this semi-passive IRS consumes power and requires a separate positioning system compared to the static reflectors, it enables dynamic and precise high-gain reflection and a variable service area.

The individual elements of the 4×4 module arrangement (total size: $40\,\mathrm{cm} \times 40\,\mathrm{cm}$) of R-HELIOS are continuously adapted mechatronically to the current position of the mobile UE by utilizing a UWB-based localization system [18], which is a widely deployed standard in the industry for localization purposes. For the resulting IRS beam tracking, which is an extension of R-HELIOS compared to its fixed beambook in [4], one UWB node is placed on top of R-HELIOS and another on the mobile STING, as depicted in Fig. 5. The latter also shows images of R-HELIOS as well as the UWB nodes and indicates the flexible service area of the reconfigurable reflector. Furthermore, the trajectory and the orientation of the mobile STING during mobility is indicated, which continuously points toward R-HELIOS to optimally utilize the reflection path via the IRS. Overall, the operation of the UWB-empowered R-HELIOS consumes at least 2.5 W (baseline) and never more than 32.3 W (peak), as measured with a power supply meter [4], which is significantly less than the energy consumption of a mmWave cell (cf. Sec. II, [14]). The functionality of the proposed RAT-external beam tracking is validated with subsequent experiments in this work.

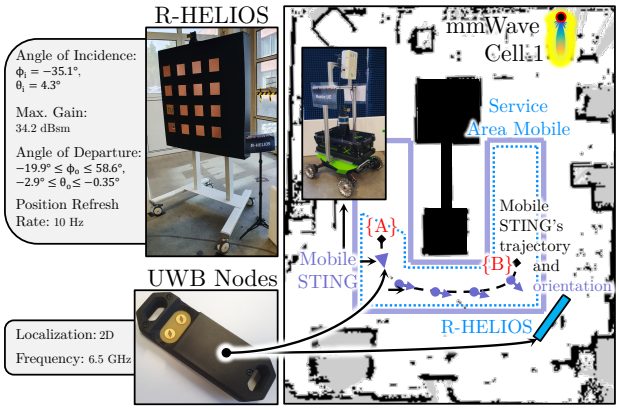

Fig. 5: Overview and setup for UWB-enabled beam tracking with R-HELIOS.

IV. Robust Network Operation with IRSs

In this section, the results of the experiments conducted are analyzed. With one of the two mmWave cells deactivated, it is first examined whether performance and connectivity in NLOS areas can be raised to a LOS-like level leveraging static-passive IRSs. Then, the validation of the proposed UWB-based beam tracking by R-HELIOS is carried out. Finally, the various options for additional network hardware are compared to derive application-specific guidance.

A. Static IRS-based mmWave Cell Compensation

To evaluate the two static-passive HELIOS reflectors, the KPIs of the three static STING devices are monitored and plotted in Fig. 6. During the measurement, only mmWave cell 1 is activated. First the top HELIOS reflector (1) and then the bottom IRS (2) are each blocked for a short time with an absorber. Initially, the three end devices measure different connectivity values due to their diverse positions. STING 3, in LOS of cell 1, achieves the highest received power of −70 dBm, whereby its PUSCH transmit power automatically reduces to a comparatively low level of −2.2 dBm. STINGs 1 and 2, both in NLOS of the mmWave cell, attain lower SS-RSRP and higher transmission power values. It is noticeable that the connectivity of STING 2 with −87 dBm is 2 dB higher than that of device 3, which arises from the different reflector designs and greater distances between UE, IRS and cell. As the reflection beam from HELIOS 1 is widened both vertically and horizontally, its reflection gain is between 9.1 dBsm and 23.1 dBsm. Due to the exclusively horizontal expansion, reflector 2 leads to gains of 15.5 dBsm to 21.8 dBsm, that being on average higher than those of IRS 1. Furthermore, it is evident that despite unequal received power values, the respective UL and DL data rates of all UEs are equally high (175 Mbit/s and 370 Mbit/s, respectively) due to their automatic transmission power adjustment. Next, when IRS 1 is blocked for 18 s, several changes occur. First, as expected, the received power of STING 1 decreases by 11 dB, whereupon its transmission power rises. Furthermore, its UL and DL data rates drop significantly to 90 Mbit/s and 146 Mbit/s, as no sufficient link to the mmWave cell can be established, hence the data path falls back to FR1. As a result, the DL throughput of devices 2 and 3 increases to 552 Mbit/s each due to the unclaimed resources in Frequency Range 2 (FR2). As soon as the absorber is removed from HELIOS 1, the initial levels of KPIs are restored. Blocking IRS 2 impacts

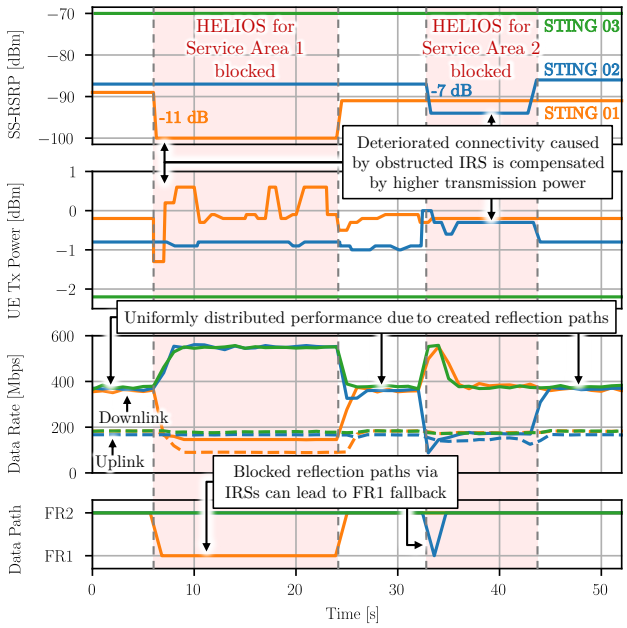

Fig. 6: Impact of HELIOS path disruption on static STING KPIs.

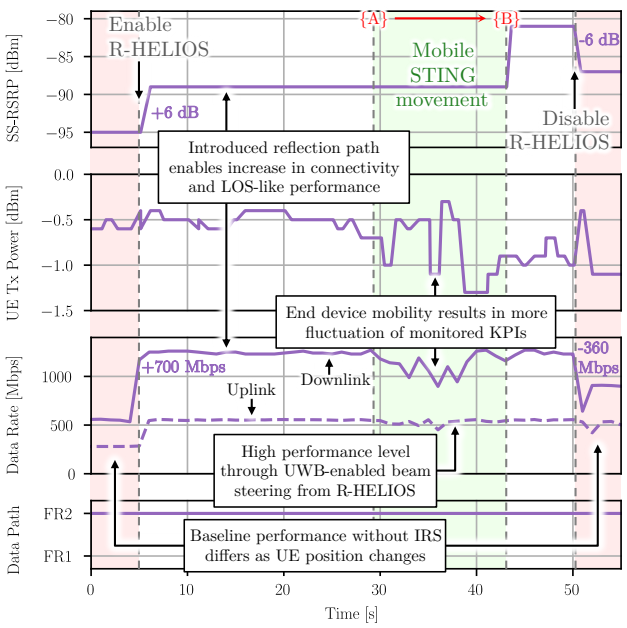

Fig. 7: Mobile STING performance with R-HELIOS integration.

STING 2 similarly. A noticeable difference is the only brief fallback of the data path, which indicates that an alternative propagation path to the cell was found, which, however, is worse than the reflection path via HELIOS, as the monitored KPIs validate. When removing the absorber, as before, the initial level of connectivity and performance is restored.

These results confirm that static HELIOS IRSs can passively enable LOS-like performance in associated service areas, allowing robust network operation and complementing earlier results on UE energy-efficiency gains [13] by demonstrating that IRS deployments can likewise improve network efficiency by enabling reduced mmWave cell density.

B. R-HELIOS-aided UE Mobility with Reduced Cell Density

While traveling the trajectory {A} to {B} (cf. Fig. 5), several KPIs are likewise monitored by mobile STING and plotted as time series in Fig. 7. At the beginning, the mobile UE stands in NLOS of active mmWave cell 1. As soon as R-HELIOS is enabled so that its reflective modules are aligned according to mobile STING's position, the newly created reflection path ensures a 6 dB higher received power and an increase in both UL and DL data rate to 570 Mbit/s and 1.27 Gbit/s, respectively. Since mobile STING is the only UE connected to mmWave cell 1 during this experiment, it can access all radio resources, so that a higher throughput can be achieved compared to the single devices in the multi-user scenario (cf. Fig. 6). As soon as the UE starts to travel the trajectory from the western to the eastern corridor ({A} to {B}) after 29 s, several effects become apparent. Firstly, the transmission power and throughput of the device fluctuate more than during standstill due to the UE's mobility. Moreover, it can be seen that the performance through the UWB-enabled beam steering from R-HELIOS remains at a high level of more than 450 Mbit/s and 900 Mbit/s in UL and DL direction. As soon as mobile STING comes to a standstill at the end of the trajectory {B}, the values stabilize again and the received power increases further by 8 dB, which hints at an optimized beam alignment of UE and mmWave cell via the reflector. When R-HELIOS is deactivated, the recorded KPIs deteriorate again, confirming the use of the reflection path via the IRS. The improved radio condition in the eastern corridor causes overall improved KPIs compared to the position in NLOS at the start of the trajectory. Although the UE is not aligned towards the cell, it is now located in LOS of cell 1 so that other, opportunistic reflection paths via metallic objects in the industrial transfer environment lead to higher connectivity than in the western corridor.

This experiment validates the UWB-enabled, semi-passive R-HELIOS IRS as an efficient solution to enhance mmWave connectivity in shadowed areas. It maintains high data rates for mobile users while achieving a large energy reduction compared to an additional mmWave cell.

C. Inter-technology Comparison of Additional RAN Hardware

The results of the evaluation enable a quantitative comparison of an additional mmWave cell and various types of IRSs in terms of average performance measurements (UL and DL) in NLOS of cell 1 as well as energy requirements examined, as shown in Fig. 8. An additional radio cell clearly provides a significant increase in both capacity and coverage, ensuring robust connectivity even in previously shadowed areas (cf. Fig. 2). However, this comes at the expense of high energy usage, increased operational costs, and additional maintenance effort, making it less favorable from an efficiency perspective.

In contrast, the static-passive IRSs do not require energy to operate, but still improve coverage in their predetermined service areas. The resulting enhanced connectivity in shadowed areas allows for more effective capacity utilization of the overall system, which makes this IRS a sustainable solution to

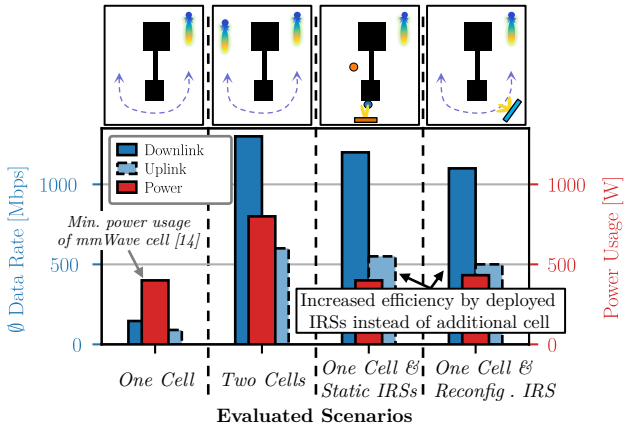

Fig. 8: Evaluation results for the investigated scenarios in NLOS of cell 1 validating Tab. I and the efficiency of IRSs over additional cell deployment.

extend network coverage. However, since preconfigured IRSs have a fixed service area which they can reasonably cover given their surface size and mounting position, they are less suitable for highly dynamic users.

Thus, the semi-passive reconfigurable IRS, R-HELIOS, was introduced in combination with UWB nodes, which facilitate positioning of the mobile user relative to the IRS. Therefore, a single IRS is enabled to flexibly adapt the mmWave coverage by optimizing its reflection pattern based on RAT-external position data. This dynamic beam tracking significantly improves coverage especially in highly dynamic use cases. While energy demand and installation cost are moderate, operational complexity is higher than for the static IRS due to the real-time beam adaptation and localization requirements.

Overall, while adding an extra cell provides the highest raw network performance, IRS-based solutions offer efficient alternatives to enhance coverage as well as performance in NLOS with lower operational cost and reduced energy consumption. The choice of IRS depends on the desired trade-off between flexibility, performance, and power usage.

V. Conclusions and Outlook

This study presented a hands-on assessment of IRS-aided mmWave networks with reduced active radio infrastructure in NLOS-constrained InF environments. While an additional mmWave cell improved the baseline connectivity and performance in shadowed zones, it also introduced significant energy usage. In contrast, with only one cell active, measurements were conducted using static-passive IRSs and the semi-passive, reconfigurable R-HELIOS reflector. The static IRSs restored LOS-like conditions in NLOS areas, enabling received power gains between 7 dB and 11 dB as well as an improved throughput in UL and DL direction, measured in a multi-user scenario, by a factor of 1.94 (from 90 Mbit/s to 175 Mbit/s) and 2.53 (from 146 Mbit/s to 370 Mbit/s), respectively, all without active power consumption. For mobile scenarios, the UWB-enabled R-HELIOS system allowed DL data rates above 900 Mbit/s (1.1 Gbit/s on average) and more than 450 Mbit/s (500 Mbit/s on average) in UL direction for a single user through adaptive beam steering. Beside its additional control complexity and power consumption in contrast to static-passive reflectors, it achieves a significant reduction in energy usage compared to deploying an additional mmWave cell.

Overall, this work shows that both static- and semi-passive IRSs can bridge coverage gaps in mmWave deployments without requiring dense active infrastructure. While static-passive, custom-tailored IRSs like HELIOS remain the most practical near-term solution, adaptive designs such as R-HELIOS constitute an important step toward flexible network deployments. In future work, the static-passive reflectors will be further investigated in industrial settings and emerging 6G test fields.

Acknowledgment

This work has been funded by the German Federal Ministry of Research, Technology and Space (BMFTR) in the course of the *6G-ANNA* project under grant no. 16KISK101, the *6GEM* research hub under grant no. 16KISK038, the *6GEM+* transfer hub under grant no. 16KIS2412, and the *PANGOLIN Networks* project under grant no. 16KIS2357.

References

[1] S. Sambhwani, H. Chae, S.-E. Chiu, B. Fan *et al.*, "Extending mmWave deployment in the next-generation network: Coverage and reliability enhancements," *IEEE Wirel. Commun.*, vol. 32, no. 1, Feb. 2025.

[2] M. Ahmed, S. Raza, A. Amin Soofi, F. Khan *et al.*, "Active reconfigurable intelligent surfaces: Expanding the frontiers of wireless communication-a survey," *IEEE Commun. Surv. Tutor.*, vol. 27, no. 2, Apr. 2025.

[3] J. Huang, C.-X. Wang, Y. Sun, R. Feng *et al.*, "Reconfigurable intelligent surfaces: Channel characterization and modeling," *Proc. IEEE*, vol. 110, no. 9, Sep. 2022.

[4] S. Häger, M. Kaudewitz, F. Schmickmann, S. Böcker *et al.*, "Field performance evaluation of a mechatronic reflector system in a private mmWave network environment," *IEEE OJ-COMS*, vol. 6, Jun. 2025.

[5] S. Häger, J. Ferreira, S. Böcker, D. Schreurs *et al.*, "Passive intelligent reflecting surfaces for efficient 6G mmWave networks: Design, validation, and field trials," *IEEE OJ-COMS*, Mar. 2026.

[6] N. Okubo, K. Tokugawa, J. Nakazato, S. Ke *et al.*, "Field evaluation of 5G mmWave relays in various topologies: NLOS coverage enhancement and tolerance against blockage," *IEEE Access*, vol. 13, May 2025.

[7] S. Prasad Tera, R. Chinthaginjala, G. Pau, and T. Hoon Kim, "Toward 6G: An overview of the next generation of intelligent network connectivity," *IEEE Access*, vol. 13, 2025.

[8] A. Tarrías, S. B. Damsgaard, M. López, T. B. Sørensen *et al.*, "Beam switching in mmWave 5G: Evaluation in a realistic industrial scenario," *IEEE Access*, vol. 12, Dec. 2024.

[9] N. González-Prelcic, M. Furkan Keskin, O. Kaltiokallio *et al.*, "The integrated sensing and communication revolution for 6G: Vision, techniques, and applications," *Proc. IEEE*, vol. 112, no. 7, Jul. 2024.

[10] RIS TECH Alliance (RISTA), "Potential Standardization Work for Reconfigurable Intelligent Surface," White Paper, Apr. 2025, version 1.0. DOI: 10.12142/FuTURE.202504003.

[11] K. Zhi, C. Pan, H. Ren, K. Wang *et al.*, "Two-timescale design for reconfigurable intelligent surface-aided massive MIMO systems with imperfect CSI," *IEEE Trans. Inf. Theory*, vol. 69, no. 5, May 2023.

[12] X. Pei, H. Yin, L. Tan, L. Cao *et al.*, "RIS-aided wireless communications: Prototyping, adaptive beamforming, and indoor/outdoor field trials," *IEEE Trans. Commun.*, vol. 69, no. 12, Dec. 2021.

[13] M. Danger, M. Khalili, S. Böcker, and C. Wietfeld, "Improving energy efficiency of industrial mmWave connectivity with context-sensitive IRS support," in *IEEE PIMRC Symp.*, Sep. 2025.

[14] O-RAN Alliance, "Network energy saving use cases," Technical Report, Jun. 2023, version 2.00, release 003. [Online]. Available: https://orandownloadsweb.azurewebsites.net/download?id=442

[15] C. Arendt, S. Böcker, C. Bektas, and C. Wietfeld, "Better safe than sorry: Distributed testbed for performance evaluation of private networks," in *Proc. IEEE FNWF Conf.*, Oct. 2022.

[16] iPerf3 - The TCP, UDP and SCTP network bandwidth measurement tool. [Online]. Available: https://iperf.fr/

[17] Wireless InSite - 3D wireless prediction software. [Online]. Available: https://www.remcom.com/wireless-insite-em-propagation-software

[18] F. Schmickmann, M. Haferkamp, J. Tiemann, and C. Wietfeld, "Bring your own positioning system: An infrastructure-free and omnidirectional UWB-based localization approach," in *Proc. IEEE VTC-Spring Conf.*, Jun. 2023.